Root electrotropism in *Arabidopsis* does not depend on auxin distribution, requires cytokinin biosynthesis and follows a power-law response curve

Nicholas Oliver[1,2,§], Maddalena Salvalaio[1,§], Deniz Tiknaz[1,3], Maximillian Schwarze[1], Nicolas Kral[1,4], Soo-Jeong Kim[1], Giovanni Sena[1,*]

[1] Department of Life Sciences, Imperial College London, UK.

[2] Present address: Department of Physics, Freie Universität Berlin, Germany.

[3] Present address: National Heart & Lung Institute, Imperial College London, UK.

[4] Present address: Phytoform Labs Ltd., Lawes Open Innovation Hub, Harpenden, UK.

[§] These authors contributed equally to this work

[*] Corresponding author

Summary

An efficient foraging strategy for plant roots relies on the ability to sense multiple physical and chemical cues in soil and to reorient growth accordingly (tropism). Root tropisms range from sensing gravity (gravitropism), light (phototropism), water (hydrotropism), touch (thigmotropism) and more[1]. Electrotropism, also known as galvanotropism, is the phenomenon of aligning growth with external electric fields and currents[2]. Although observed in a few species[3–5] since the end of the 19th century[6], the molecular and physical mechanism of root electrotropism remains elusive, limiting the comparison to more defined sensing pathways in plants.

Here we provide a first quantitative and molecular characterisation of root electrotropism in the model system *Arabidopsis thaliana,* showing that it does not depend on an asymmetric distribution of the plant hormone auxin, but that instead it requires the biosynthesis of a second hormone, cytokinin. We also show that the dose-response kinetics of root electrotropism follows a power law analogous to the one observed in common animal physiological reactions[7], suggesting universal properties.

A full molecular and quantitative characterisation of root electrotropism would represent a step forward towards a better understanding of signal integration in plants, and an independent outgroup for comparative analysis of electroreception in animals[8] and fungi[9].

Introduction

Plant roots navigate the complex soil environment in search of water and nutrients, through various sensing mechanisms reorienting their growth towards or away from signal sources (tropism)[1]. For example, hydrotropism redirects growth towards high moisture[10], (negative) phototropism redirects away from light sources[11], and gravitropism induces growth downwards, following the gravity vector[12]. The integration of overlapping and frequently contradicting molecular and physical signals is as critical for plant roots as it is for other soil organisms.

Although many molecular aspects of a few root tropisms have been understood[1], several key sensing mechanisms remain elusive. One of these is the capacity of plant roots to sense electric fields (electrotropism or galvanotropism)[2]. The reception of electric fields (electroreception) has been observed in vertebrates[8] and invertebrates[13], including common model systems such as *C. elegans*[14] and *Dyctostylium*[15], as well as in fungi[9]. Interestingly, electric sensing structures have been identified only in a few aquatic animal species[16] and more recently in bumble-bees[17].

First recorded in 1882[6] and rediscovered at the start of the 20th century[18], root electrotropism has been studied sporadically in maize (*Zea mays*), peas (*Pisum sativum*) and bean (*Vigna mungo*) but with contradicting results[3–5]. Crucially, the anatomical and molecular details of sensing electric fields are still largely unknown in roots. A quantitative description of root electrotropism's kinetics is also missing, preventing a comparative analysis with animal electroreception and electrotaxis.

Results

A novel root electrotropism assay

To study for the first time root electrotropism in the plant model system *Arabidopsis thaliana,* we developed a new setup to stimulate, image and quantitate electrotropism in its primary root. Briefly, roots were grown vertically in a transparent chamber (V-box) containing a buffered liquid medium and two immersed electrodes connected to a power supply to generate a uniform electric field and an ionic current perpendicular to the growing roots (Fig. 1a and Methods).

To maintain constant temperature and minimise the pH gradient generated by electrolysis, the liquid medium was continuously circulated in a closed loop between the V-box, a cooled water bath and a 2-litre reservoir bottle (Extended Data Fig. 1 and Methods). In each V-box, the primary roots of five seedlings were imaged every 10 minutes with a camera mounted in front of the V-box (Extended Data Fig. 1a and Methods). We measured the actual field generated in the medium by immersing voltmeter probes in the two neighbouring positions of each seedling: as expected, the field measured in the medium was lower than the nominal imposed in air between the two electrodes, but still relatively uniform across the five positions (Extended Data Fig. 2a). At the same time, we measured the current passing through the circuit

(Extended Data Fig. 2b and Methods).

To quantify the root response to the applied electric field, we took an image of the roots every 10 minutes and measured the angle between the root tip and the vertical gravity vector (Fig. 1b).

To confirm that the circulation of the liquid medium was effective in damping any pH gradient created by electrolysis and in eliminating any chemotropic effect, we imposed a field of 1.5 V/cm in a V-box without plants for one hour while maintaining liquid circulation. We then turned off the field and the liquid circulation, immediately positioned the plants in the V-box and imaged the roots for the next 80 minutes: we did not observe any significant deviation in root growth direction (t-test between 1.5 V/cm and no field at 80 m, $p=0.964$), compared to roots in a V-box that never experienced the electric field (Extended Data Fig. 2c), indicating that no significant pH gradient was left in the medium.

Root tip reorientation in an external electric field

We measured the response of wild-type (WT) *Arabidopsis* primary roots to a continuous electric field. The distribution of reorientations to a range of fields intensities between 0.5 V/cm and 2.5 V/cm shows a quick tropism towards the negative electrode, or cathode (Fig. 1c).

We wondered how much of this effect was due to trivial electrostatic, *i.e.* the physical force perceived in the field by a hypothetical excess of positive charges on the root, as opposed to a more complex biological phenomenon. To address this, we pre-treated the roots in a 50 °C bath until growth and gravitropism were suppressed, transferred to the V-box and exposed them to a 2.0 V/cm electric field (Methods): the root response shows that this simple treatment was sufficient to completely inhibit electrotropism when compared to roots kept at a standard 23 °C temperature (t-test between 50 °C and 23 °C at 5 h, $p<0.001$), strongly suggesting that electrostatic alone could not explain the root response and that this is, in fact, a biological phenomenon (Extended Data Fig. 3).

Response curves

The progressively sharper root tip reorientation as the field intensity was increased (Fig. 1c) suggests that the sensing mechanism is not acting as a simple on/off switch but that it can distinguish electric fields of different strengths. To quantitate this, we plotted the orientation angle at 5 h ("response") as a function of the electric field intensity ("stimulus"), and found the best fit with a power function with exponent 0.45 (Fig. 2a, left), indicating that the resolution of the sensor is higher at low-intensity stimuli (steep response curve) than at high-intensity stimuli (shallow response curve). The analogous response curve as a function of the measured current intensity is best fit with a power function with exponent 0.33 (Fig. 2a, right). Interestingly, power-law response curves with similar exponents have been traditionally measured in physiological responses to external stimuli in animal systems[7]: our results suggest that a power-law response to external stimuli might be a universal feature across life kingdoms, and that it does not require a nervous system. Moreover, it might reveal constraints on the

genetic architecture of the underlying sensory system[19].

Since the root tip reorientations did not show any obvious overshoot (Fig. 1c), we looked more closely at the angular velocity: the maximum average velocity in WT roots was reached when the root tip was between 10 and 20 degrees orientation to the gravity vector (Fig. 2b), and then progressively decreased as the root tip approached its maximum reorientation (Fig. 2b). This indicates that the mechanism can sense and respond differently to the changing relative orientation of the tip with the external electric field, and to progressively slow down the root tip rotation as it approaches the target orientation. Moreover, the maximum angular velocity appears to be roughly proportional to the electric field strength (Fig. 2c, left), although this is much less evident as a function of the electric current (Fig. 2c, right).

Root tips are not damaged

Early reports noted that protracted exposure to external fields could cause physical damage to plant root tips[20]. To control whether this was the case in our experimental conditions, we developed a simple chambered slide (V-slide) to be mounted on a standard confocal microscope stage (Extended Data Fig. 4a and Methods) with electrodes on the chamber's sides and a circulating liquid medium for temperature control similar to the one implemented in the V-box (Extended Data Fig. 4b). Seedlings from the *Arabidopsis* transgenic line constitutively expressing the yellow fluorescent cell-membrane marker WAVE 131Y [21] were mounted on the V-slide and imaged at cellular resolution while exposed to a 1.0 V/cm electric field (Methods). The field of view in our time-lapse images comprises the meristem, the transition zone and the distal elongation zone, but no cellular pattern perturbation was noticeable in any of these regions when compared to roots not exposed to the field (Extended Data Fig. 5).

Also, the time-lapse suggests that asymmetric cell expansion in the elongation zone is causing the bending, as expected from other examples of root tropism[22].

Regions of competence

Since the root bending occurs in the elongation zone, we wanted to identify the region responsible for sensing the electric field. We excised distal fragments of the root at 125 µm, 300 µm, 400 µm and 500 µm from the tip (Fig. 3a), and then exposed the cut root to 1.5 V/cm (Methods).

In the first 2 h (Fig. 3b left), roots cut at 400 µm from the tip turned to angles indistinguishable from uncut roots exposed to the same field (Wilcoxon between 400 µm cut and uncut at 1.5 V/cm at 2 h, $p=0.211$), while roots cut at 500 µm from the tip did not turn and at 2 h showed orientations indistinguishable from uncut roots not exposed to a field (t-test between 500 µm cut at 1.5 V/cm and uncut at 0 V/cm at 2 h, $p=0.164$). These results indicate that the 400 µm distal fragment is not necessary for the early (2 h) electrotropic response, while the 500 µm distal fragment is; since the elongation zone involved in the bending spans an extended region proximal to the 500 µm cut, we conclude that in *Arabidopsis* roots the region between 400 µm and 500 µm from the tip is necessary for early sensing an external electric

field.

Between 2 h and 5 h of exposure (Fig. 3b right), while roots cut at 300µm on average continue to turn like the uncut roots (t-test between 300 µm cut and uncut at 1.5 V/cm at 5 hrs, p=0.071), roots cut at 400 µm quickly fail to sustain their response and at 5 h they show tip orientations on average different than those of uncut roots exposed to the same field (t-test between 400 µm cut and uncut at 1.5V/cm at 5 hrs, p<0.001). These results indicate that the 300 µm distal fragment is not necessary to maintain the electrotropic response up to 5hrs, while the 400 µm distal fragment is; we conclude that in *Arabidopsis* roots the region between 300 µm and 400 µm from the tip is necessary for prolonged sensing of the imposed electric field.

Interestingly, previous studies suggested that the movement of Ca++ ions accumulated in the mucilage at the very tip of the root might be involved in the electrotropic sensing[23]. Since any excision above 125 µm from the tip essentially removes all the mucilage from the root, our results disprove this hypothesis for *Arabidopsis*.

Auxin distribution is not altered by the electric field

The fact that roots without tips could still respond to the electric field shows that even a major disruption of the stereotypical auxin redistribution mechanism is not sufficient to inhibit electrotropism.

On the other hand, an asymmetric accumulation of auxin is required for asymmetric cell elongation and root bending in some tropisms, as suggested by the classic Cholodny-Went model[24]. To test whether this model applied to electrotropism and whether the external electric field is sufficient to induce an asymmetric distribution of auxin in the root, we exposed roots expressing the auxin-sensitive fluorescent reporter *R2D2*[25] to a field of 1.0 V/cm for 30 minutes, before quickly mounting them on a microscope slide and imaging them with a confocal microscope (Methods). A ratiometric quantification of *R2D2* signal in each epidermal cell (Fig. 4a; Extended Data Fig. 6 and Methods) showed that the average auxin response measured in the epidermal cells on the side facing the negative electrode and on the side facing the positive electrode were statistically indistinguishable (Fig. 4b; Methods), both in the distal (Wilcoxon test, p=0.696) and the proximal (Wilcoxon test, p=0.843) region of the root, indicating that auxin is not asymmetrically distributed after exposure to the electric field.

Moreover, both sides were also indistinguishable from the average between the two sides in roots not exposed to the field (mock), both in the distal (Wilcoxon test between the negative exposed side and mock, p=0.775; and between the positive exposed side and mock, p=0.881) and in the proximal (Wilcoxon test between the negative exposed side and mock, p=0.041; and between the positive exposed side and mock, p=0.098) regions.

Auxin transport is not necessary for early response

Previous work indicated that auxin transport inhibitors can inhibit electrotropism response in maize roots[3]. To verify this in *Arabidopsis,* and further explore the role of auxin in root electrotropism, we used N-1-naphthylphthalamic acid (NPA) to inhibit polar auxin transport[26]

while exposing the roots to the electric field. We tested 0.1 μM, 1.0 μM and 10 μM NPA and found that 10 μM NPA was the lowest concentration of NPA to inhibit gravitropism (Methods), a known auxin-dependent tropism.

We pre-treated the seedlings for 3 hours in liquid medium containing 10 μM NPA (Methods) and then transferred them to a V-box containing 10 μM NPA in the medium and the reservoir. In the first 2 hours of field exposure (Fig. 4c left) the NPA-treated roots reoriented at angles indistinguishable from those of untreated ones (Wilcoxon test between NPA-treated and mock at 2 h, $p=0.684$). From 2 to 5 hours of exposure (Fig. 4c right), NPA-treated roots seemed to return to a more vertical orientation compared to untreated roots, although not in a statistically significant way due to very large variance (t-test between NPA-treated and mock at 5 h, $p=0.094$). These results indicate that auxin polar transport is not necessary for an early electrotropic response, but might play a role in maintaining a long-term orientation.

To further explore the role of auxin transport, we tested the mutants of PIN2, an auxin cellular exporter[27], and mutants of AUX1, an auxin cellular importer[28]. Since *pin2* and *aux1* mutants do not respond to gravity, to obtain a sufficient number of roots growing vertically in preparation for the electrotropic assay, we wrapped the bottom part of the nursery boxes with aluminium foil to induce negative root phototropism towards the bottom of the box (Methods). The same setup was used to germinate WT plants to be compared with these to mutants.

Roots of *pin2* mutants (Fig. 4d) showed a significant response (paired Wilcoxon between the time-points 0 h and 2 h, $p<0.01$; and between the time-points 0 h and 5 h, $p<0.01$), but weaker than WT (t-test between WT and *pin2* at 2 h, $p<0.01$; and between WT and *pin2* at 5 h, $p<0.01$) in the same conditions. Their angular velocity did not show an obvious decrease before reaching the target orientation, as with WT roots (Fig. 2b).

Analogously, roots of *aux1* mutants (Fig. 4d) showed a significant early response (paired t-test between the time-points 0 h and 2 h, $p<0.01$), but weaker than WT (t-test between WT and *pin2* at 2 h, $p<0.01$; t-test between WT and *pin2* at 5 h, $p<0.01$) in the same conditions. Interestingly, *aux1* roots on average failed to maintain their orientation for a longer period (paired t-test between the time-points 0 h and 5 h, $p=0.051$). Moreover, their angular velocity on average decreased while approaching the final orientation, as with WT roots (Fig. 2b).

Taken together, these results suggest that although auxin transport seems to play a role in maintaining a sustained response to the electric field, it is not necessary for triggering early electrotropism.

Cytokinin biosynthesis is necessary for electrotropism

Root hydrotropism, or the growth towards high concentration of water, was also previously shown to be largely independent of auxin distribution in *Arabidopsis*[29], while it requires biosynthesis and asymmetric distribution of cytokinin[30], another plant hormone.

Given our results suggesting a limited role for auxin during electrotropism, we wondered if a cytokinin-dependent pathway similar to that involved in hydrotropism might play a role in electrotropism as well. We tested mutants of two genes required for the cytokinin-dependent hydrotropic response: *cyp735a1,* a cytochrome P450 monooxygenase enzyme necessary for

the biosynthesis of the *trans*-zeatine variation of cytokinin[31] and for root hydrotropism[30], and *mizu-kussein1* (*miz1*), necessary for cytokinin asymmetric distribution in *Arabidopsis* roots[30] and for hydrotropism[32].

Roots of *cyp735a1* mutants (Fig. 4e) failed to respond to the electric field, with tip orientations indistinguishable from that of WT roots not exposed to the field (t-test between *cyp735a1* exposed to 1.5 V/cm and WT not exposed at 5 h, p=0.748), showing that cytokinin biosynthesis is necessary for electrotropism in *Arabidopsis* roots.

Interestingly, roots of *miz1* mutants (Fig. 4e) showed an unperturbed electrotropic response in the first 2 h (Wilcoxon test between *miz1* and WT at 2 h, p=0.859) and perhaps a weakened response at 5 h, although not statistically significant (t-test between *miz1* and WT at 5 h, p=0.033), suggesting that the asymmetric distribution of cytokinin is not necessary for electrotropism.

Taken together, these surprising results indicate that cytokinin plays an important, although still unknown, role in root electrotropism.

Discussion

The capability of plant roots to sense and combine numerous physical and chemical signals in the soil is quite extraordinary, notably in the absence of a centralised processing system. The more we understand about the physical and molecular mechanism behind the various root tropisms, the closer we will get to a complete understanding of signal integration in plants. In this work, we focused on the little-studied phenomenon of root electrotropism and present its first quantitative characterization in the flowering plant model system *Arabidopsis thaliana.*

A non-trivial observation from this work is that plant roots respond to weak (order of 1 V/cm and 100 μA) external electric fields and currents in a progressive way, with an increasingly stronger tendency to align with the field as the field and current intensities increase. This is interesting because it reveals a sophisticated way to discriminate between highly charged particles (*e.g.* ions, micro-organisms, other plant roots) and weakly charged ones. At the same time, the absence of overshooting also points to a mechanism that perhaps can be modelled along the lines of a proportional–integral–derivative control system[33]. Moreover, we show that the kinetics (response curve) of root electrotropism follows a power-law reminiscent of the Stevens law used to describe physiological responses in animal biosensors[7], which could shed some light on the underlying genetic network[19] and at the same time suggest the existence of universal classes of biosensing mechanisms spanning across biological kingdoms.

A second, perhaps unexpected, result from this work is the identification of two regions in *Arabidopsis* roots required for the detection of the field: the section between roughly 400 μm and 500 μm from the tip is necessary for the early detection (within 2 h from exposure), while the section between roughly 300 μm and 400 μm is necessary for a prolonged detection (up to 5 h from exposure). Interestingly, these sections seem to correspond to the well-characterised anatomical transition zone, between the meristem and the elongation zone in roots, which has

been previously involved in root sensing[1,34]. In future works, it will be crucial to discern whether the electrotropism mechanism depends on a relatively large region like the transition zone or if it can be narrowed to a more specific cell population therein.

Finally, we present evidence against the assumption that auxin asymmetric distribution is required for electrotropism in *Arabidopsis*, similarly to what found for hydrotropism[29] and phototropism[35]. Instead, we suggest that cytokinin plays a role, although future studies will have to investigate its role even further.

References

1. Muthert, L. W. F., Izzo, L. G., Zanten, M. van & Aronne, G. Root Tropisms: Investigations on Earth and in Space to Unravel Plant Growth Direction. *Front Plant Sci* **10**, 1807 (2020).

2. Navez, A. E. Galvanotropism of roots. *The Journal of general physiology* **10**, 551–558 (1927).

3. Ishikawa, H. & Evans, M. L. Electrotropism of maize roots. Role of the root cap and relationship to gravitropism. *Plant physiology* **94**, 913–918 (1990).

4. Stenz, H. G. & Weisenseel, M. H. Electrotropism of Maize (Zea-Mays L) Roots - Facts and Artifacts. *Plant physiology* **101**, 1107–1111 (1993).

5. Wolverton, C., Mullen, J. L., Ishikawam, H. & Evans, M. L. Two distinct regions of response drive differential growth in Vigna root electrotropism. *Plant Cell Environ* **23**, 1275–1280 (2000).

6. Elfving, F. Ueber eine Wirkung des galvanischen Stromes auf wachsende Wurzeln. *Bot. Zeit.* 257–264 (1882).

7. Stevens, S. S. Neural Events and the Psychophysical Law: Power functions like those that govern subjective magnitude show themselves in neurelectric effects. *Science* **170**, 1043–1050 (1970).

8. Crampton, W. G. R. Electroreception, electrogenesis and electric signal evolution. *J Fish Biol* **95**, 92–134 (2019).

9. McGillivray, A. M. & Gow, N. A. R. Applied Electrical Fields Polarize the Growth of Mycelial Fungi. *Microbiology* **132**, 2515–2525 (1986).

10. Miyazawa, Y. & Takahashi, H. Molecular mechanisms mediating root hydrotropism: what we have observed since the rediscovery of hydrotropism. *J Plant Res* **133**, 3–14 (2019).

11. Kutschera, U. & Briggs, W. R. Root phototropism: from dogma to the mechanism of blue light perception. *Planta* **235**, 443–452 (2012).

12. Su, S.-H., Gibbs, N. M., Jancewicz, A. L. & Masson, P. H. Molecular Mechanisms of Root Gravitropism. *Current Biology* **27**, R964–R972 (2017).

13. Clarke, D., Whitney, H., Sutton, G. & Robert, D. Detection and learning of floral electric fields by bumblebees. *Science* **340**, 66–69 (2013).

14. Sukul, N. C. & Croll, N. A. Influence of potential difference and current on the electrotaxis of Caenorhaditis elegans. *J Nematol* **10**, 314–7 (1978).

15. Shanley, L. J., Walczysko, P., Bain, M., MacEwan, D. J. & Zhao, M. Influx of extracellular Ca2+ is necessary for electrotaxis in Dictyostelium. *J Cell Sci* **119**, 4741–4748 (2006).

16. Peters, R. C., Eeuwes, L. B. M. & Bretschneider, F. On the electrodetection threshold of aquatic vertebrates with ampullary or mucous gland electroreceptor organs. *Biol Rev* **82**, 361–373 (2007).

17. Sutton, G. P., Clarke, D., Morley, E. L. & Robert, D. Mechanosensory hairs in bumblebees (Bombus terrestris) detect weak electric fields. *Proceedings of the National Academy of Sciences* **113**, 7261–7265 (2016).

18. Ewart, A. J. & Bayliss, J. S. On the nature of the galvanotropic irritability of roots. *Proc Royal Soc Lond Ser B Contain Pap Biological Character* **77**, 63–66 (1905).

19. Adler, M., Mayo, A. & Alon, U. Logarithmic and Power Law Input-Output Relations in Sensory Systems with Fold-Change Detection. *Plos Comput Biol* **10**, e1003781 (2014).

20. Wawrecki, W. & Zagórska-Marek, B. Influence of a Weak DC Electric Field on Root Meristem Architecture. *Ann Bot-london* **100**, 791–796 (2007).

21. Geldner, N. *et al.* Rapid, combinatorial analysis of membrane compartments in intact plants with a multicolor marker set. *The Plant journal : for cell and molecular biology* **59**, 169–178 (2009).

22. Gilroy, S. Plant tropisms. *Current Biology* **18**, R275-7 (2008).

23. Marcum, H. & Moore, R. Influence of Electrical Fields and Asymmetric Application of Mucilage on Curvature of Primary Roots of Zea mays. *American Journal of Botany* **77**, 446 (1990).

24. Thimann, K. V. & Went, F. W. *Phytohormones*. (1937). doi:10.5962/bhl.title.5695.

25. Liao, C.-Y. *et al.* Reporters for sensitive and quantitative measurement of auxin response. *Nature methods* **12**, 207–210 (2015).

26. Sabatini, S. *et al.* An auxin-dependent distal organizer of pattern and polarity in the Arabidopsis root. *Cell* **99**, 463–472 (1999).

27. Chen, R. *et al.* The Arabidopsis thaliana AGRAVITROPIC 1 gene encodes a component of the polar-auxin-transport efflux carrier. *Proc National Acad Sci* **95**, 15112–15117 (1998).

28. Marchant, A. *et al.* AUX1 regulates root gravitropism in Arabidopsis by facilitating auxin uptake within root apical tissues. *Embo J* **18**, 2066–2073 (1999).

29. Shkolnik, D., Krieger, G., Nuriel, R. & Fromm, H. Hydrotropism: Root Bending Does Not Require Auxin Redistribution. *Mol Plant* **9**, 757–759 (2016).

30. Chang, J. *et al.* Asymmetric distribution of cytokinins determines root hydrotropism in Arabidopsis thaliana. *Cell Res* **29**, 984–993 (2019).

31. Takei, K., Yamaya, T. & Sakakibara, H. Arabidopsis CYP735A1 and CYP735A2 Encode Cytokinin Hydroxylases That Catalyze the Biosynthesis of trans-Zeatin. *J Biol Chem* **279**, 41866–41872 (2004).

32. Kobayashi, A. *et al.* A gene essential for hydrotropism in roots. *Proc Natl Acad Sci U S A* **104**, 4724–4729 (2007).

33. Chevalier, M., Gómez-Schiavon, M., Ng, A. H. & El-Samad, H. Design and Analysis of a Proportional-Integral-Derivative Controller with Biological Molecules. *Cell Syst* **9**, 338-353.e10 (2019).

34. Baluška, F., Mancuso, S., Volkmann, D. & Barlow, P. W. Root apex transition zone: a signalling–response nexus in the root. *Trends in Plant Science* **15**, 402–408 (2010).

35. Kimura, T. *et al.* Asymmetric Auxin Distribution is Not Required to Establish Root Phototropism in Arabidopsis. *Plant Cell Physiology* **59**, 828–840 (2018).

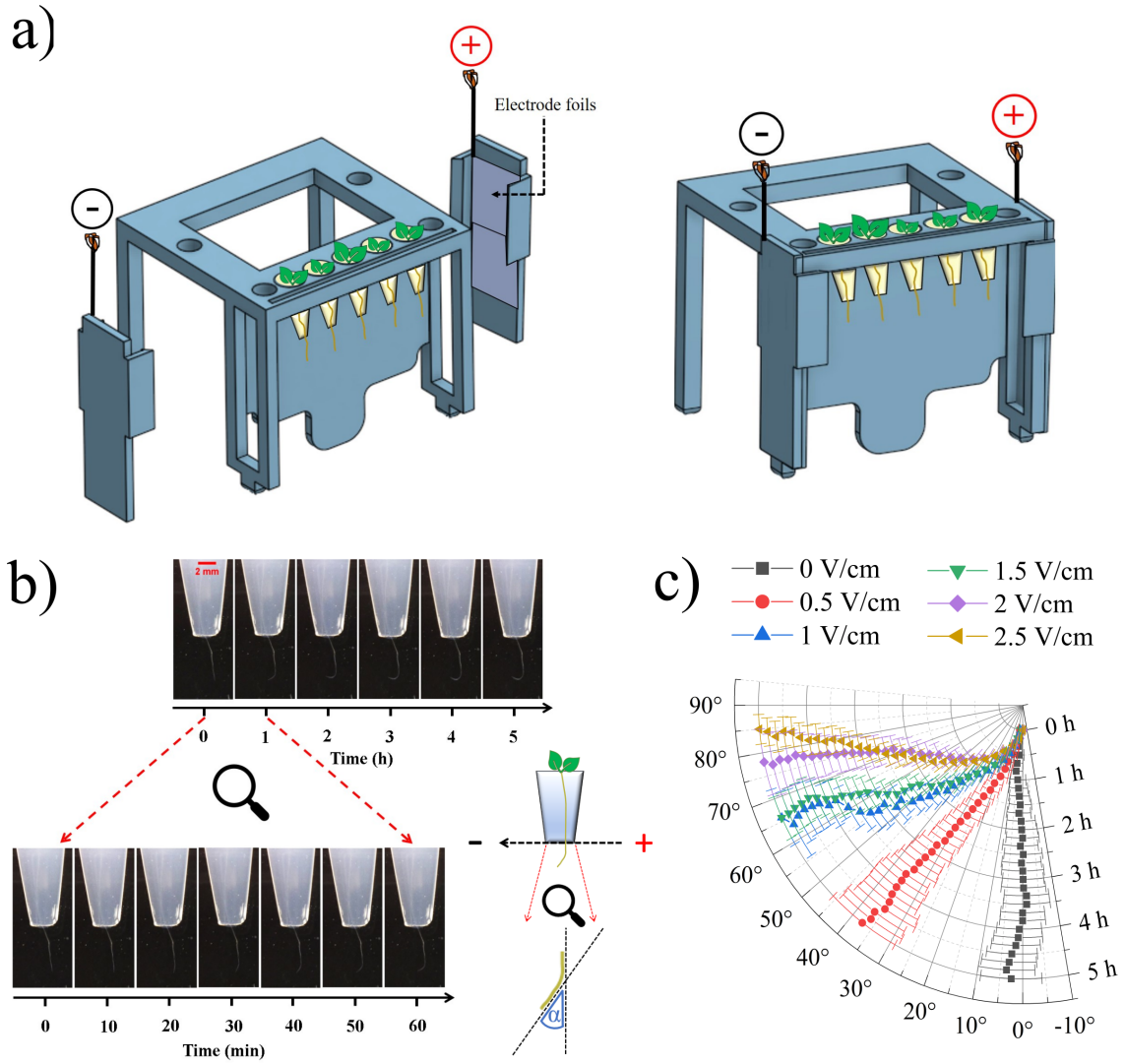

Fig. 1

a, Schematic of the 3D-printed module used in the V-box. **b,** Time-lapse series of a single root as imaged by the Raspberry camera from the V-box. **c,** Polar plot of the average root tip orientations relative to the gravity vector, with time on the radial axis and orientation angle on the circumferential axis; error bars, s.e.m. **d,** Schematic of the angle measured and plotted in c.

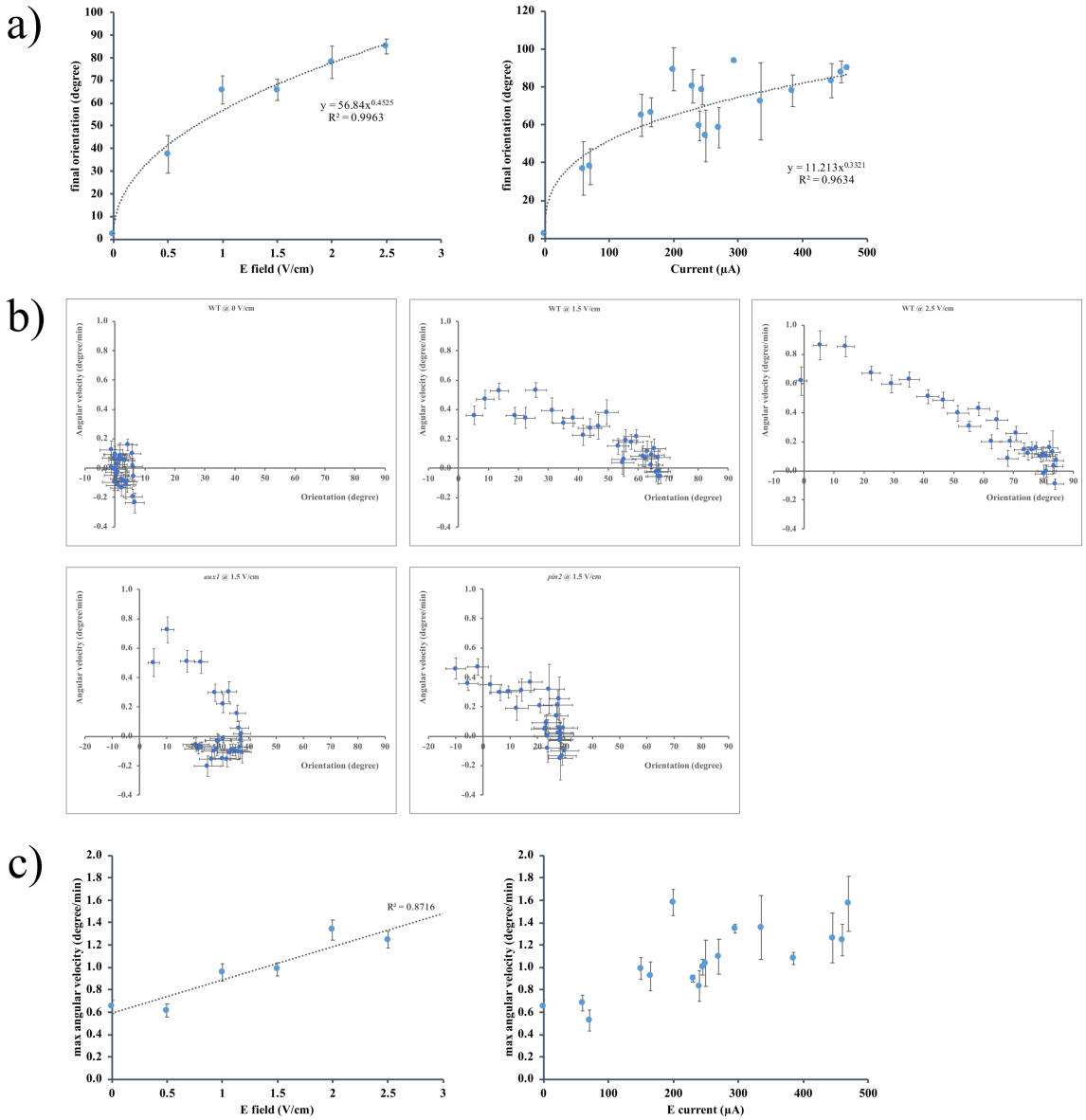

Fig. 2

a, Root electrotropism response curves: average root tip orientations at 5hrs vs. electric field (left panel) or current (right panel); error bars, s.e.m.; R^2, coefficient of determination. **b,** Top row: root tip average angular velocity at any observed orientation, for 0 V/cm (left panel), 1.5 V/cm (middle panel) and 2.5 V/cm (right panel); Bottom row: same plots for the mutants *aux1* (left panel) and *pin2* (right panel) at 1.5 V/cm; error bars, s.e.m. **c,** Average maximum angular velocity reached by the root tip at a given electric field (left) or current (right); error bars, s.e.m.; R^2, coefficient of determination.

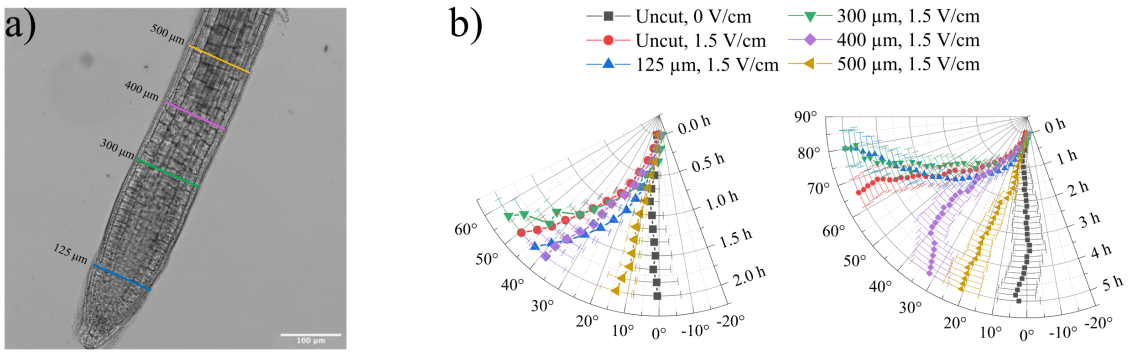

Fig. 3

a, Points of excision overlapped to a microscope image of the *Arabidopsis* primary root tip; scale bar, 100 µm. **b,** Polar plot of the average root tip orientations relative to the gravity vector, with time on the radial axis and orientation angle on the circumferential axis; error bars, s.e.m.

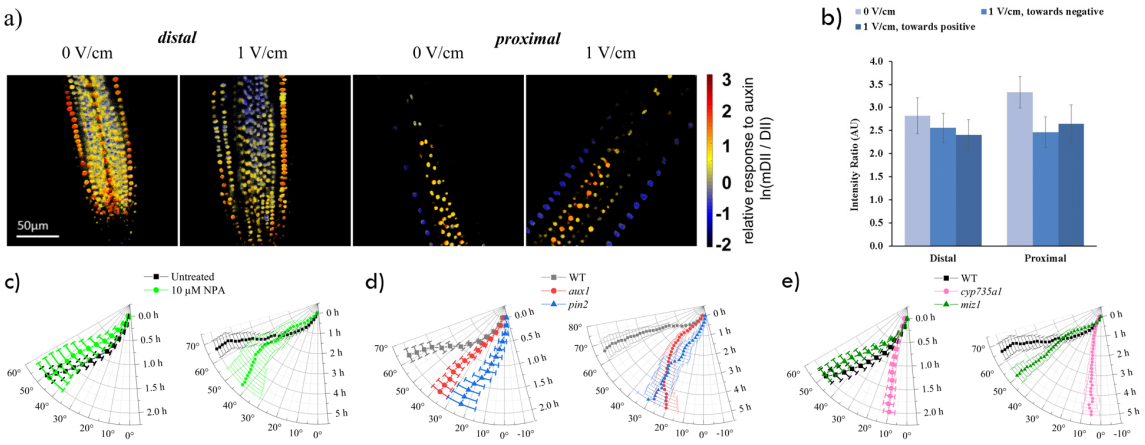

Fig. 4

a, Root tip images colour-coded to show the relative response to auxin concentration, as measured by the ratiometric fluorescent reporter R2D2 (see Methods); left panels: representative tip (distal) regions at 0 V/cm and 1 V/cm; right panels: representative higher (proximal) regions at 0 V/cm and 1 V/cm; scale bar, 50µm. **b,** Quantification of the average relative response to auxin (as shown in a) in the epidermis cell layer facing the anode or cathode, in the distal and proximal regions; the data for 0 V/cm is an average between the two sides; error bars, s.e.m. **c-e,** Polar plots of the average root tip orientations relative to the gravity, exposed to 1.5 V/cm, with time on the radial axis and orientation angle on the circumferential axis: NPA-treated (**c**), *aux1* and *pin2* (**d**), *cyp735a1* and *miz1* (**d**), ; error bars, s.e.m.

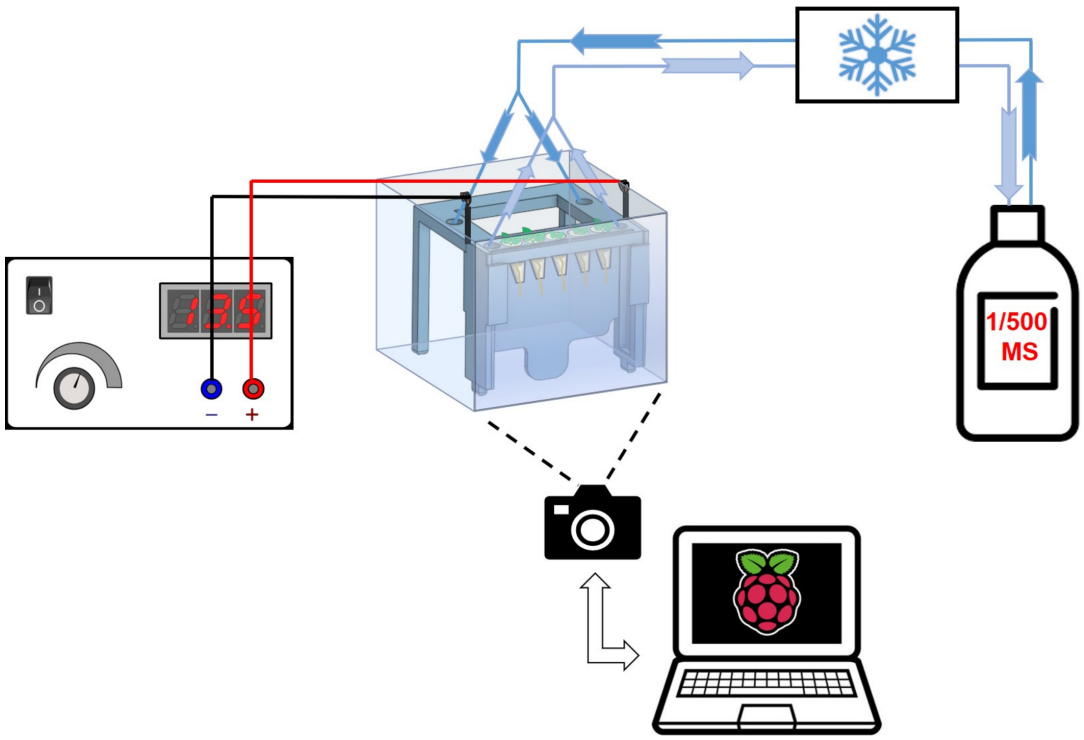

Extended Data Fig. 1
Diagram of the complete setup used for the electrotropism assay.

a)

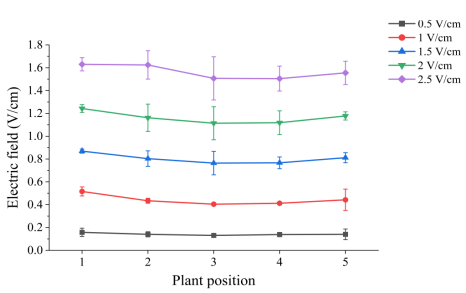

b)

Electric field (V/cm)	Current (µA)
0.5	65.5 ± 5.8
1	157.5 ± 7.9
1.5	247.7 ± 13.3
2	264.7 ± 78.8
2.5	438.5 ± 40.8

c)

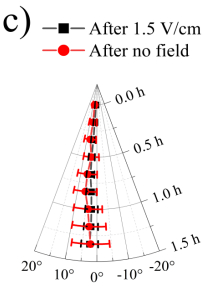

Extended Data Fig. 2

a, Average electric field measurements inside the V-box at each of the five plant positions (N=3 measurements), for each voltage difference imposed by the power supply between the electrodes; error bars, s.e.m. **b,** Average (+/- standard deviation) electric currents measured in the circuit for each voltage difference imposed by the power supply between the electrodes. **c,** Control for efficient circulation of the liquid medium: polar plot of the average root tip orientations relative to the gravity vector, with time on the radial axis and orientation angle on the circumferential axis, of unexposed roots inside a V-box that had been pre-exposed to 1.5 V/cm or 0 V/cm (see main text); error bars, s.e.m.

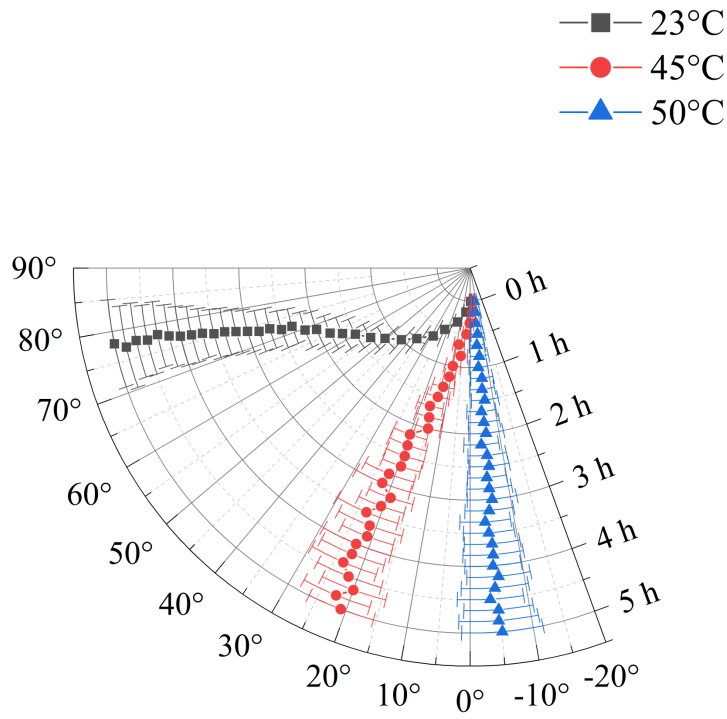

Extended Data Fig. 3

Polar plot of the average root tip orientations relative to the gravity vector, with time on the radial axis and orientation angle on the circumferential axis, for roots pre-treated to 23 °C, 45 °C or 50 °C and then exposed to 2.0 V/cm; error bars, s.e.m.

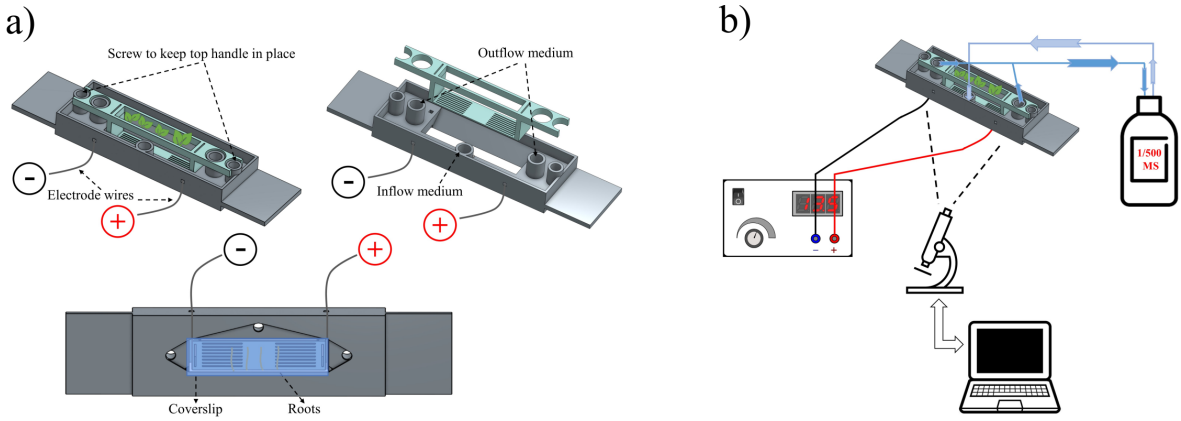

Extended Data Fig. 4

a, Diagram of the V-slide used to image with confocal microscopy a root exposed to the electric field. **b,** Diagram of the complete setup used with the V-slide.

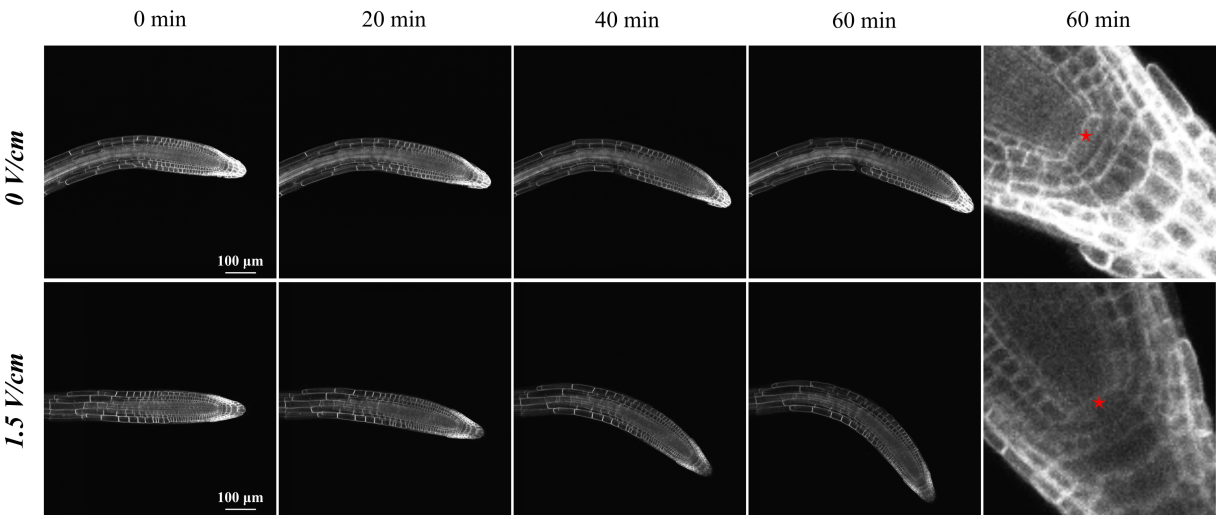

Extended Data Fig. 5

Time-lapse confocal images of two representative roots (total roots observed: N=3 for mock and N=3 for 1.5 V/cm) expressing the WAVE131Y marker, exposed to 0 V/cm or 1.5 V/cm in the V-slide; red star, the quiescent centre (QC); scale bars, 100 µm.

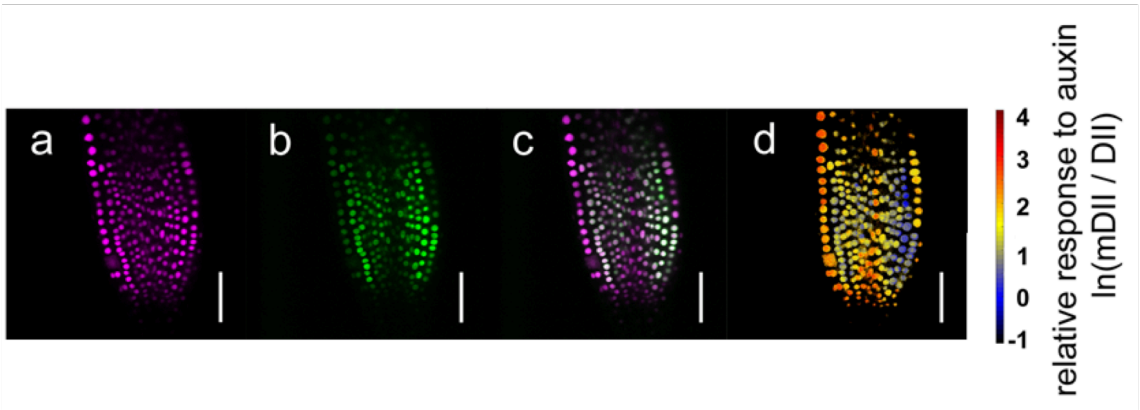

Extended Data Fig. 6

R2D2 two-channel image collection and conversion into a ratiometric image. **a,** Signal collected from the non-degradable mDII::ntdTomato; **b,** Signal collected from the degradable DII:n3xVenus; **c,** Overlay image of the two channels. **d,** Ratio image of the two channels, higher ratio indicates higher auxin. Values for the colours used in the ratio image are shown next to the colour bar, standing for the relative response to auxin ln(mDII fluorescence/DII fluorescence). Scale bars, 50 µm.

Methods

Plant material

Wild-type and mutant *Arabidopsis thaliana* plants were all from the Columbia (Col-0) ecotype; the following mutant alleles were used: *aux1-7* (NASC id 9583) for *aux1*, *eir1-1* (NASC id 8058) for *pin2, miz1-2* for *miz1* (NASC id N576560) and *cyp735a1* (NASC id N593028). The fluorescent line *WAVE131Y* is expressing *pUBQ10::WAVE131:YFP* (NASC id N781535); the fluorescent line *R2D2* is expressing *RPS5A-mDII-ntdTomato, RPS5A-DII-n3xVenus* (courtesy of Dr Teva Vernoux).

Seeds were imbibed in water and kept in the dark for 2 days at 4 °C to synchronise germination. All seeds were surface sterilised using 50% Haychlor bleach and 0.0005% Triton X-100 for 3 minutes and then rinsed 6 times with sterilised milliQ water. Seed germination protocols are described in the experiment-specific Methods sections below. All experiments were conducted on with primary roots of seedlings 5-8 days post-germination.

Electrotropism assay (V-box)

Seeds were sown individually inside PCR tubes filled with 1X MS gel medium: 0.44% Murashige and Skoog (MS) Basal medium (Sigma-Aldrich, M5519), 0.5% sucrose, 0.05% MES hydrate (Sigma-Aldrich M8250), 0.8% agar (Sigma-Aldrich 05040), pH adjusted to 5.7 with TRIS HCl (Fisher-Scientific 10205100). The PCR tubes had their end cut out to allow the root to grow through, and placed in a 3D-printed (Ultimaker 2+) holder inserted in a Magenta box (Sigma-Aldrich V8380). The Magenta box was filled with 150 ml of 1/500X MS liquid medium (0.00088% MS Basal medium, 0.5% sucrose, 0.05% MES hydrate, pH5 adjusted to 5.7 with TRIS HCl) to reach the end of the PCR tubes. These “germination” or “nursery” boxes were placed in a growth chamber at 23 °C, with a 16 h/8 h light/dark photoperiod and light intensity 120 µmol m^{-2} s^{-1}

In preparation for the electrotropism assay, each PCR tube containing a single 7 to 10-day-old seedling was transferred to a modified 3D-printed holder in a Magenta box filled with 1/500X MS liquid medium. The modified module consisted of a main body with five holes for the PCR tubes containing the seedlings, and two side clips to position the electrodes consisting of platinum-iridium (Platinum:Iridium = 80:20; Alfa Aesar 41805.FF) foils (Fig. 1a), which were connected to an external power supply. In this paper, we refer to the Magenta box and its holder as the “V-box”. In addition to the five holes for the plants, four extra holes were designed on the stand: two at each end of the front side to pump the medium out of the V-box, and two more on the back to pump the medium in, using a tubing system and peristaltic pumps (Verdeflex AU R2550030 RS1) to circulate the medium at a speed of 1 ml/sec to and from a 2 l reservoir bottle (Extended Data Fig. 1). Crucially, between the V-box and the reservoir bottle, the tubings were immersed in a cooled water bath (Grant Instruments, LTDGG) maintained at the constant temperature of 19 °C (Extended Data Fig. 1), which was enough to maintain the

medium inside the v-box at a constant 23 °C, as measured. All electrotropic experiments were performed at constant illumination.

The electric field was generated with a power supply attached to the platinum-iridium foil electrodes that were immersed in the liquid medium in the V-box. Standard electric wires were soldered on the top of two electrodes, always kept outside the liquid medium to avoid contaminants from the solder. The voltage was set constant on the power supply, while the current was measured independently with a multimeter in series.

To record the movement of the roots over time, a Raspberry Pi camera module V2 (913-2664) connected to a Raspberry Pi board module B+ (137-3331) was used. The Raspberry Pi was programmed to take a picture every 10 minutes, using the command *crontab* in the local Raspbian OS.

WT electrotropism assays were performed with the following sample sizes: 0 V/cm, N=10; 0.5 V/cm, N=9; 1.0 V/cm, N=8; 1.5 V/cm, N=21; 2.0 V/cm, N=18; 2.5 V/cm, N=20.

Mutants electrotropism assays were performed with the following sample sizes: *aux1*, N=18; *pin2*, N=13; *cyp735a1*, N=20; *miz1*, N=9.

The control for medium circulation efficiency was performed with the following sample sizes: 1.5 V/cm, N=5; 0 V/cm, N=10.

High-temperature treatment

Wild-type Col-0 seeds were germinated and grown for 7 to 10 days in the nursery boxes as described in the Electrotropism Assay section. The boxes undergoing treatment were then immersed in a water bath set at 45 °C or 50 °C, for 10 minutes. The PCR tubes containing the seedlings were then transferred to a V-box, exposed to an electric field of 2.0 V/cm for 5 hours and imaged, as described in the Electrotropism Assay section.

Electrotropism assays for excised roots were performed with the following sample sizes: 23°C, N=18; 45°C, N=5; 50°C, N=5.

For the gravitropism control, seedlings were treated with high temperature as described above and then transferred on 1X MS agar plates, to complete the assay as described in the Gravitropic Assay section.

Electrotropism on a microscope (V-slide)

Seeds of the transgenic reporter line *WAVE131Y* (see Plant Material section) were germinated on 1X MS agar medium (0.44% MS Basal medium, 0.5% sucrose, 0.05% MES hydrate, pH adjusted to 5.7 with TRIS HCl, 0.8% agar) in square plates kept vertical in a growth chamber at 22 °C, with a 16 h/8 h light/dark photoperiod.

At 2 days post-germination the seedlings were mounted on the V-slide with 1/500X MS liquid medium (0.00088% MS Basal medium, 0.5% sucrose, 0.05% MES hydrate, pH5 adjusted to 5.7 with TRIS HCl). The V-slide was then connected to the medium perfusion system circulating the same 1/500X MS medium, and the V-slide's electrodes were connected to the power supply (Voltcraft PS-1302-D).

Imaging was performed on a Leica SP5 laser scanning confocal microscope with 20X air objective, while the liquid medium was circulated and the electric field maintained constant. Fluorophore was excited with the 514 nm Argon laser line and the emission collected with PMT detector at 524-570 nm. Images were collected at intervals of 2 minutes.

Root tip excisions

Seeds were germinated in nursery boxes as described.

At 3 days post-germination, seedlings were transferred to hard 1X MS agar medium (0.44% MS Basal medium, 0.5% sucrose, 0.05% MES hydrate, pH adjusted to 5.7 with TRIS HCl, 5.0% agar) and manually dissected using a dental needle (Sterican, 27G) under a dissecting microscope (Nikon SMZ1000) at 180X magnification, following the published protocol {Kral, 2009}.

After root tip excision, the seedlings were immediately moved into the V-box for the electrotropism assay.

Electrotropism assays on excised roots were performed with the following sample sizes: 125 µm, N=16; 300 µm, N=7; 400 µm, N=10; 500 µm, N=10; uncut at 0 V/cm, N=10; uncut at 1.5 V/cm, N=21.

R2D2 reporter

Seeds of the transgenic reporter line *R2D2* (see Plant Material section) were germinated in nursery boxes and exposed to 1.0 V/cm for 30min in V-boxes, as described in the Electrotropism Assay section. After exposure, *R2D2* roots were quickly mounted on standard microscope slides with sterile deionised water and imaged using Leica SP5 laser scanning confocal microscope, with 63X water immersion objective.

R2D2 expresses two versions of a protein that forms a complex with auxin: DII-n3xVENUS, which is degraded within minutes upon binding with auxin; mDII-ntdTOMATO, which contains a modified, non-degradable, version of DII. Both of the proteins are localised in the nucleus. We followed the published protocol[25] to separately collect the emission from mDII-ntdTOMATO (Extended Data Fig. 6a) and DII-n3xVENUS (Extended Data Fig. 6b).

For each root, a mean background was defined as the average pixel intensity in the mDII channel of an 80x80 pixels corner of the field of view not occupied by the root. The mean background was then subtracted from all pixel intensities in both channels (mDII and DII). We manually segmented with FIJI{Schindelin:2012ir} the most visible cell nuclei in the epidermis of each root, both in the distal (12 roots in mock conditions and 16 roots exposed to the field) and in the proximal (11 roots in mock conditions and 13 roots exposed to the field) regions of the root tip, and quantified the average pixel intensity (corrected after background subtraction) for each segmented nucleus. Finally, we calculated the natural log of the ratio between the average mDII (non-degradable, auxin-independent) and DII (degradable, auxin-dependent) signals in each nucleus and mapped it on top of the root image (Extended Data Fig. 6d).

For each root, we calculated the average and standard deviation of these ratios, for

epidermal nuclei facing the anode or the cathode (Fig. 4b).

Sample size as following: exposed to E field and imaged in the distal region, N=16; exposed to E field and imaged in the proximal region, N=13; not exposed to E field and imaged in the distal region, N=24; not exposed to E field and imaged in the proximal region, N=22.

NPA treatment

To find the minimum concentration of N-1-naphthylphthalamic acid (NPA) that inhibits gravitropism, seeds were germinated on 1X MS agar medium (0.44% MS Basal medium, 0.5% sucrose, 0.05% MES hydrate, pH adjusted to 5.7 with TRIS HCl, 0.8% agar) and at 3 days post-germination were transferred for 3 hrs into cell culture dishes containing 5 ml of 1/500X MS liquid medium (0.00088% MS Basal medium, 0.5% sucrose, 0.05% MES hydrate, pH5 adjusted to 5.7 with TRIS HCl) plus NPA at 0.1 µM, 1.0 µM and 10 µM. The seedlings were then transferred onto 1/500X MS agar plates (0.00088% MS Basal medium, 0.5% sucrose, 0.05% MES hydrate, pH5 adjusted to 5.7 with TRIS HCl, 0.8% agar) containing the same concentration of NPA. The plates were moved to a growth room (22 °C, 16 h/8 h light/dark photoperiod), rotated by 90 degrees and monitored for root gravitropic response.

To quantify the effect of NPA on electrotropism, after being treated with a concentration of 10 µM NPA for 3 hours as described above, the seedlings were transferred inside a V-box and exposed to a 1.5 V/cm electric field as described in the Electrotropism Assay section. Both the V-box and the reservoir bottle contained 10 µM NPA throughout the experiment.

Samples sizes were the following: mock-treated, N=21; 10 µM NPA treated, N=8.

Gravitropism assay

Seeds were germinated on 1X MS agar medium (0.44% MS Basal medium, 0.5% sucrose, 0.05% MES hydrate, pH adjusted to 5.7 with TRIS HCl, 0.8% agar) in square plates kept vertical in a growth chamber at 22°C, with a 16 h/8 h light/dark photoperiod and light intensity 120 µmol m^{-2} s^{-1}

At 3 days post-germination the plates were rotated by 90 degrees, and the root tips monitored for gravitropic response in the following 24 h.

Statistical analysis

When comparing two samples of measurements, each distribution was first checked for normality with the Shapiro-Wilk test with alpha-level = 0.05. Normal distributions were tested with the two-tails Student's t-test without assuming equal variances (Welch two-sample t-test); if one of the two distributions was not normal, the non-parametric Mann-Whitney U (Wilcoxon) test was used. Unless stated otherwise, all comparisons were performed assuming independence (unpaired test). All statistical tests were performed with R.

Acknowledgements

We thank T. Vernoux for providing seeds of the *R2D2* line; A. Guyon, O. Kranse, C. Keyzor, C.D. Livesey-Clare for generous technical help; M. Levin and I. Bordeu for critical discussions at various stages of the project. This work was partly supported by the BBSRC Impact Acceleration Account BB/S506667/1 and the Allen Discovery Center at Tufts University; N.K. was supported by the BBSRC DTP grant BB/M011178/1.

Author Contributions

N.O., M.Sa. and G.S. conceived and designed the experiments. N.O. and M.Sa. performed most of the electrotropism assays and analysed the data, and contributed to the development of the V-box. D.T. contributed to the development of the V-slide and performed some of the electrotropism assays. M.Sc. performed the root excision experiments and the electrotropism assays for *cyp735a1*, and analysed the data. N.K. contributed to the development of the V-slide and performed the *R2D2* and *WAVE131Y* imaging. S.J.K. performed the heat-treatment experiments. M.Sc. and G.S. prepared the manuscript, with all the authors contributing to the Methods section.

Competing interests

The authors declare no competing interests.

Additional information

Correspondence and requests for materials should be addressed to G.S.